The all particle energy spectrum of KASCADE-Grande in the energy region 10^{16} - 10^{18} eV by means of the N_{ch} - N_{μ} technique

M. Bertaina[‡], W.D. Apel[*], J.C. Arteaga[†,xi], F. Badea[*], K. Bekk[*], J. Blümer[*,†], H. Bozdog[*] I.M. Brancus[§], M. Brüggemann[¶], P. Buchholz[¶], E. Cantoni[‡,‖], A. Chiavassa[‡], F. Cossavella[†], K. Daumiller[*], V. de Souza[†,xii], F. Di Pierro[‡], P. Doll[*], R. Engel[*], J. Engler[*], M. Finger[*], D. Fuhrmann[**], P.L. Ghia[‖], H.J. Gils[*], R. Glasstetter[**], C. Grupen[¶], A. Haungs[*], D. Heck[*], J.R. Hörandel[†,xiii], T. Huege[*], P.G. Isar[*], K.-H. Kampert[**], D. Kang[†], D. Kickelbick[¶], H.O. Klages[*], P. Łuczak[††], H.J. Mathes[*], H.J. Mayer[*], J. Milke[*], B. Mitrica[§], C. Morello[‖], G. Navarra[‡], S. Nehls[*], J. Oehlschläger[*], S. Ostapchenko[*,xiv], S. Over[¶], M. Petcu[§], T. Pierog[*], H. Rebel[*], M. Roth[*], H. Schieler[*], F. Schröder[*], O. Sima[‡‡], M. Stümpert[†], G. Toma[§], G.C. Trinchero[‖], H. Ulrich[*], A. Weindl[*], J. Wochele[*], M. Wommer[*], J. Zabierowski[††]

[*]*Institut für Kernphysik, Forschungszentrum Karlsruhe, 76021 Karlsruhe, Germany*
[†]*Institut für Experimentelle Kernphysik, Universität Karlsruhe, 76021 Karlsruhe, Germany*
[‡]*Dipartimento di Fisica Generale dell'Università, 10125 Torino, Italy*
[§]*National Institute of Physics and Nuclear Engineering, 7690 Bucharest, Romania*
[¶]*Fachbereich Physik, Universität Siegen, 57068 Siegen, Germany*
[‖]*Istituto di Fisica dello Spazio Interplanetario, INAF, 10133 Torino, Italy*
[**]*Fachbereich Physik, Universität Wuppertal, 42097 Wuppertal, Germany*
[††]*Soltan Institute for Nuclear Studies, 90950 Lodz, Poland*
[‡‡]*Department of Physics, University of Bucharest, 76900 Bucharest, Romania*
[xi]*now at: Universidad Michoacana, Morelia, Mexico*
[xii]*now at: Universidade de São Paulo, Instituto de Fîsica de São Carlos, Brasil*
[xiii]*now at: Dept. of Astrophysics, Radboud University Nijmegen, The Netherlands*
[xiv]*now at: University of Trondheim, Norway*

***Abstract*. The KASCADE-Grande experiment, located at Forschungszentrum Karlsruhe (Germany) is a multi-component extensive air-shower experiment devoted to the study of cosmic rays and their interactions at primary energies 10^{14} - 10^{18} eV. One of the main goals of the experiment is the measurement of the all particle energy spectrum in the 10^{16} - 10^{18} eV region. For this analysis the Grande detector samples the charged component of the air shower while the KASCADE array provides a measurement of the muon component. An independent fit of the lateral distributions of charged particle and muon densities allows to extract the charged particle and muon sizes of the shower. The size of the charged particles, combined with the ratio between charged particle and muon sizes, which is used to take into account shower-to-shower fluctuations, is used to assign the energy on an event-by-event basis, in the framework of the CORSIKA-QGSjetII model. The method itself, and the energy spectrum derived with this technique are presented.**

***Keywords*: Energy spectrum, KASCADE-Grande, 10^{16} - 10^{18} eV**

I. INTRODUCTION

The KASCADE-Grande experiment [1] is a multi-component air-shower experiment with the aim of measuring the all particle energy spectrum in the 10^{16} - 10^{18} eV region by sampling the charged particle and muon densities. A fit to the lateral distribution of the charged particle densities allows to reconstruct the shower parameters (core position, angular direction) and the size of the charged component (see [2] for details). An independent fit of the lateral distribution of the muon densities (see [3],[4]), gives the size of the muon component of the shower. The performance of the KASCADE-Grande array, and, therefore, its high accuracy up to energies 10^{17} -10^{18} eV, essential to derive an accurate energy spectrum, is summarized in [2].

The conversion between the observed quantities (charged particle and muon sizes) of the Extensive Air Shower (EAS) to the energy of the primary particle requires the assumption of a specific hadronic interaction model, whose suitability has to be verified beforehand. In this work, the energy estimations are based on the CORSIKA-QGSjetII model [5], [6], motivated by the fact that such model reproduces fairly well the distributions of the ratio of the muon and electron sizes measured by KASCADE-Grande as a function of both the electron size and the atmospheric depth [7].

The method described in this paper uses the combined information of the charged particle and muon sizes on an event-by-event basis, with the aim of reducing the systematics on the primary composition in the energy assignment, systematics which are the main sources of uncertainty on methods based on a single component

information ([4], [8]).
The analysis presented here is based on ∼981 days of data collected on the central area of KASCADE-Grande array (∼0.2 km^2) at zenith angles $\theta < 40^\circ$ corresponding to a total acceptance $A = 2.50 \cdot 10^9$ cm$^2\cdot$ sr (exposure $E = 2.12 \cdot 10^{17}$ cm$^2\cdot$ s·sr).

II. TECHNIQUE

The technique has been defined on simulated data assuming a power law with index γ=-3 for the energy spectrum and then applied to the experimental ones. Proton and iron nuclei have been selected as primaries, to represent the two extreme cases. The simulation includes the full air shower development in atmosphere, the response of the detector and its electronics, as well as their uncertainties. Therefore, the reconstructed parameters from simulated showers are obtained exactly in the same way as for real data. Data have been subdivided in 5 angular bins of same acceptance ($\theta <$ 16.7, 16.7 $\leq \theta <$ 24.0, 24.0 $\leq \theta <$ 29.9, 29.9 $\leq \theta <$ 35.1, 35.1 $\leq \theta <$ 40.0) and the analysis is conducted independently in each angular bin. The difference in the results obtained among the angular bins will be considered as one of the sources in the final systematic uncertainty on the energy spectrum. In this way, possible differences in the air shower attenuation in atmosphere (i.e. the zenith angle) between real and simulated data, will be included directly into the systematic uncertainties of the measurement, without applying any correction. The energy assignment is defined as $E = f(N_{ch}, k)$ (see eq. 1), where N_{ch} is the size of the charged particle component and the parameter k is defined through the ratio of the sizes of the N_{ch} and muon (N_μ) components: $k = g(N_{ch}, N_\mu)$ (see eq. 2). The main aim of the k variable is to take into account the average differences in the N_{ch}/N_μ ratio among different primaries with same N_{ch}, and the shower to shower fluctuations for events of the same primary mass:

$$log_{10}(E[GeV]) = [a_p + (a_{Fe} - a_p) \cdot k] \cdot log_{10}(N_{ch}) + \\ + b_p + (b_{Fe} - b_p) \cdot k \quad (1)$$

$$k = \frac{log_{10}(N_{ch}/N_\mu) - log_{10}(N_{ch}/N_\mu)_p}{log_{10}(N_{ch}/N_\mu)_{Fe} - log_{10}(N_{ch}/N_\mu)_p} \quad (2)$$

where,

$$log_{10}(N_{ch}/N_\mu)_{p,Fe} = c_{p,Fe} \cdot log_{10}(N_{ch}) + d_{p,Fe}. \quad (3)$$

The coefficients a, b, c, d are obtained through the fits to the scatter plots ($N_{ch}, N_{ch}/N_\mu$) and (N_{ch}, E) in the region $6 < log_{10}(N_{ch}) < 8$, which means above the ∼100% trigger efficiency, and up to the energy for which the simulated statistics is sufficiently high. The k parameter is, by definition of eq. 2, a number centered around 0 for a typical proton shower and 1 for a typical iron shower. As an example, figs. 1 and 2 show such scatter plots for the iron component in the 1^{st} angular bin. Similar plots are obtained in the other 4 angular bins as well as for proton primaries.

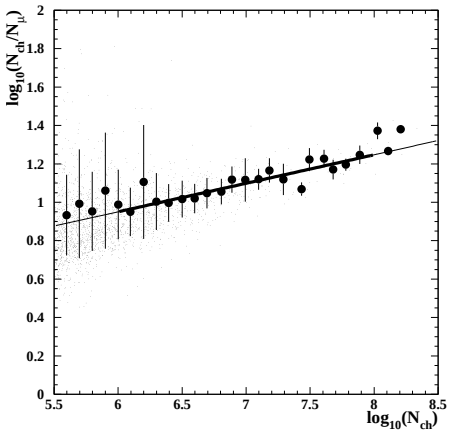

Fig. 1: Scatter plot of N_{ch}/N_μ vs N_{ch} for primary iron nuclei. The small dots indicate single events, while full ones refer to the average values in each N_{ch} interval (ΔN_{ch} = 0.1). The error bar of the full dots indicates the RMS of the distribution of the small dots in each N_{ch} interval. The linear fit is performed on the full dots and their uncertainties in the region $6 < log_{10}(N_{ch}) < 8$ (thick line). Such fit is used to obtain the parameters c and d of expression 3.

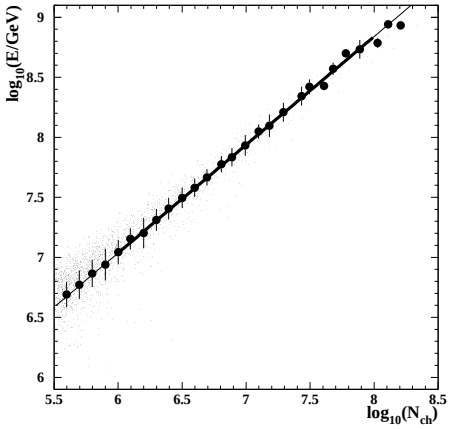

Fig. 2: Scatter plot of E vs N_{ch} for iron primary nuclei. See fig. 1 for detailed explanation of the meaning of dots and error bars. The fit is used to obtain the parameters a and b of expression 1.

In order to check the capability of this technique of correctly reproducing the original energy spectrum, the expressions 1 and 2 have been applied to: a) the simulated energy spectra they have been derived from (H and Fe); b) to other three mass groups (He, C, Si) simulated using the same criteria; c) to the mixture of the five mass groups with 20% abundance each. Fig. 3 shows a comparison between the reconstructed and true energy spectra obtained for the 1^{st} angular bin in case of iron primary nuclei. Similar plots are obtained for the other mass groups and for all angular bins. Fig. 4 summarizes

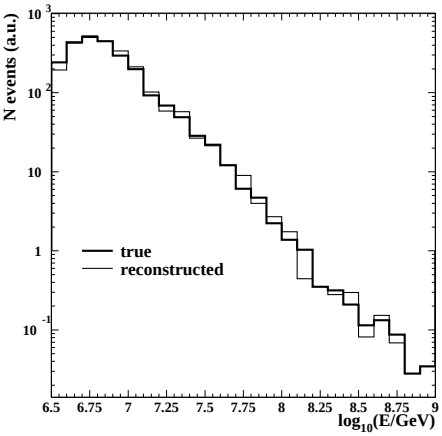

Fig. 3: True (thick line), and reconstructed (thin line) energy spectrum in the 1^{st} angular bin for iron primary nuclei according to expressions 1 and 2.

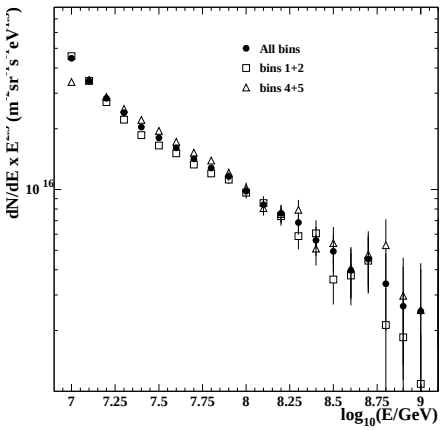

Fig. 5: The experimental energy spectrum (differential intensity multiplied by $E^{2.5}$) as a function of $\log_{10}$(E/GeV) for vertical (bins 1+2), more inclined (bins 4+5) and all events (only statistical uncertainties).

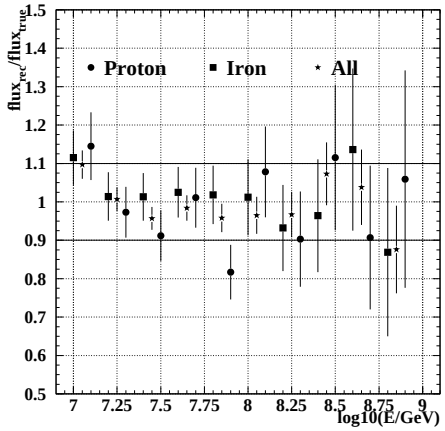

Fig. 4: Ratio between the reconstructed and true spectra (as shown in fig. 3) for protons, iron and all mixed primaries (all angular bins together).

the results on the ratio between reconstructed and true spectra for protons, iron and all mixed primaries. The original energy spectra are fairly well reproduced. The systematic uncertainties are discussed in section III.

III. The reconstructed energy spectrum and its uncertainties

Expressions 1 and 2 have been applied to the experimental data obtaining the intensities shown in fig. 5. A detailed analysis of the systematic uncertainties on the intensities has been conducted taking into account the following effects:

a) Systematic uncertainty from the comparison of the intensity in different angular bins.
b) Systematic uncertainty on the $E(N_{ch})$ relation.
c) Systematic uncertainty related to the capability of reproducing an, *a priori* assumed, single primary spectrum with slope γ = -3 (i.e. difference between true and reconstructed spectra of fig. 3).
d) Systematic uncertainty on the muon lateral distribution function (l.d.f.).

Possible systematic uncertainties on the reconstructed N_{ch} and N_{μ} values compared to the true ones, are already taken into account by the technique itself as the same reconstruction procedure is applied to simulated and real data.

Concerning a), in fig. 5 data points of the 1^{st} and 2^{nd} angular bins have been summed together, and the same for data of the 4^{th} and 5^{th} bins. The semi-difference of the intensity in each energy interval (subtracted from the statistical uncertainty) between vertical and more inclined angular bins provides an estimation of the uncertainty on the relative energy calibration among the angular bins, together with the systematic uncertainty related to possible differences in the air shower attenuation in the atmosphere between real and simulated data. At E $\sim 10^{17}$ ($\sim 3 \cdot 10^{16}$) eV (at higher energies the results are dominated by the statistical uncertainty) the systematic uncertainty is $\sim$5% ($\sim$15%). This result confirms the fact that the technique is self-consistent in the entire angular range used in this analysis and that the QGSjetII model reproduces quite consistently the shower development at least up to zenith angles $\theta < 40$ degrees. The uncertainty on the intensity provides only an indication on the relative uncertainty among expressions 1 and 2 for different angular bins, but doesn't take into account a common systematic effect of all $E = f(N_{ch}, k)$. For this reason, $E = f(N_{ch}, k)$ in simulated data have been artificially modified, at a level in which the systematic effect is clearly visible between the true and reconstructed simulated energy spectra as in fig. 3 and an upper limit has been set and used as systematic effect on the $E(N_{ch})$ conversion relation: at E $\sim 10^{17}$ eV such uncertainty is $< 10\%$.

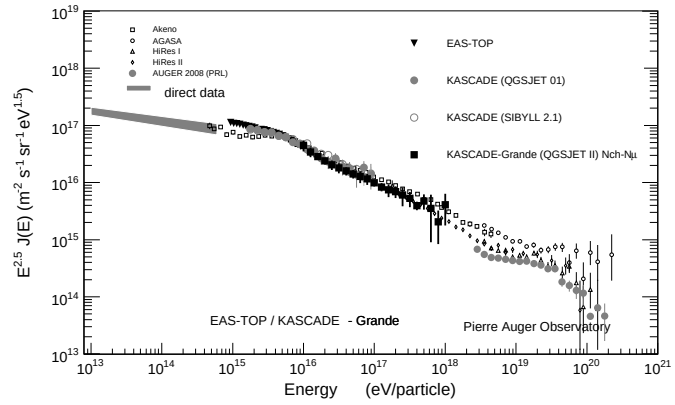

Fig. 6: All primaries energy spectrum (intensity multiplied by $E^{2.5}$) obtained with KASCADE-Grande data applying the N_{ch} - N_{μ} technique. A comparison with other experimental results is also presented.

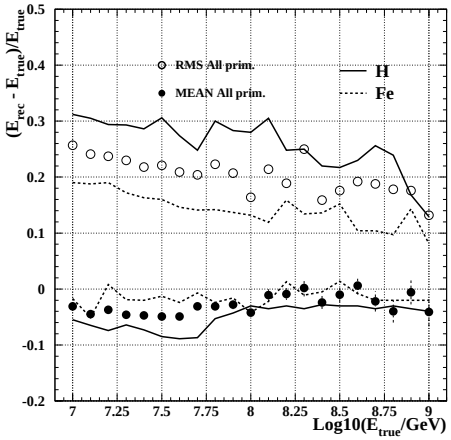

Fig. 7: Resolution in the energy assignment for a mixture of primaries of the 5 simulated mass groups (relative abundance of each group 20%), for H and Fe. The full dots show the offset of the reconstructed energy E_{rec} in bins of true energy E_{true}. The open dots show the RMS of such distributions (see text for details).

A further systematic uncertainty comes from the capability of reproducing the original energy spectrum assuming a single mass composition as shown in fig. 4. In general the ratio between the reconstructed and true fluxes obtained in each energy bin are compatible, inside the statistical uncertainty, with unity. Only at the threshold a systematic effect of $\sim$12% is visible. The typical relative differences in flux at energies E$<10^{17}$ eV are $<$5%.

Regarding d), the energy spectrum has been obtained for different ranges of distance of the shower core from the muon detector. The relative difference in intensity as a function of energy is used to compute a systematic uncertainty due to the assumed l.d.f., and it amounts to $\sim$3% at E $\sim$ 10^{17}, slightly increasing with energy.

Finally, it is interesting to look at the relative uncertainty in the energy assignment on an event-by-event basis. Simulated data using the mixture of all primaries have been divided in bins of true energy (E_{true}) and the distributions of the relative differences between reconstructed (E_{rec}) and true energies have been created. As shown in fig. 7 the RMS of such distributions (energy resolution) is $\sim$26% at the energy threshold and decreases with energy, due to the lower fluctuations of the shower development, becoming $<$ 20% at the highest energies. The small offset in the mean values of the distributions at low energies is necessary to take into account the effect of shower fluctuations on a steep spectrum. Such offset does not appear in fig. 4, which indicates that the correct energy spectrum is well reproduced. Results for pure H and Fe primaries are also indicated by lines.

The statistical uncertainty on the intensity is $<$10% up to E$\sim 3 \cdot 10^{17}$ eV. The total uncertainty (statistical and systematic squared together) on the intensity is $<$20% at energies E $< 10^{17}$ eV in the frame of the CORSIKA-QGSjet model.

IV. Results

The all particle energy spectrum of KASCADE-Grande in the 10^{16} - 10^{18} eV energy region using the N_{ch} - N_{μ} technique is shown in fig. 6. The uncertainty in each intensity point is obtained as squared sum of all systematic and statistical uncertainties. At the threshold, the spectrum overlaps well with KASCADE and EAS-TOP spectra. Moreover, it is in agreement with the energy spectra of KASCADE-Grande obtained using other techniques ([4], [8], [9]) which have partially different systematic uncertainties (see [10]).

The mean of the average $\overline{k}$ obtained in different bins of N_{ch} in the range $6 < log_{10}(N_{ch}) < 8$ is $< \overline{k} >$ = 0.64, with bin to bin fluctuations of $\sigma_{\overline{k}} \sim$ 0.06, therefore, perfectly compatible with the limits set by eq. 2 using QGSjetII simulations.

References

[1] G. Navarra et al. - KASCADE-Grande Collaboration, Nucl. Instr. and Meth. A 518 (2004).
[2] F. Di Pierro et al. - KASCADE-Grande Collaboration, These Conference Proceedings.
[3] D. Fuhrmann et al. - KASCADE-Grande Collaboration, These Conference Proceedings.
[4] J.C. Arteaga et al. - KASCADE-Grande Collaboration, These Conference Proceedings.
[5] D. Heck et al. Forschungszentrum Karlsruhe, Report FZKA 6019 (1998).
[6] S. Ostapchenko, *QGSjetII:results for extensive air showers*, astro-ph/0412591.
[7] E. Cantoni et al. - KASCADE-Grande Collaboration, These Conference Proceedings.
[8] D. Kang et al. - KASCADE-Grande Collaboration, These Conference Proceedings.
[9] G. Toma et al. - KASCADE-Grande Collaboration, These Conference Proceedings.
[10] A. Haungs et al. - KASCADE-Grande Collaboration, These Conference Proceedings.